Near-infrared InGaAs FPAs for space applications

GONG Hai-mei[1], TANG Heng-jing[1,2], LI Xue[1], ZHANG Ke-feng[1,2], LI Yong-fu[1,2],

LI Tao[1,2], NING Jin-hua[1,2], WANG Yang[1], MIAO Guo-qing[3], SONG Hang[3],

ZHANG Yong-gang[4], FANG Jia-xiong[1]

(1.State Key Laboratories of Transducer Technology, Shanghai Institute of Technical Physics, Chinese Academy of Sciences, Shanghai 200083, China; 2.Graduate School of the Chinese Academy of Sciences, Beijing 100039, China; 3.Key Laboratory of Excited State Processes, Changchun Institute of Optics, Fine Mechanics and Physics, Chinese Academy of Sciences, Changchun 130033, China; 4.State Key Laboratory of Functional Materials for Informatics, Shanghai Institute of Microsystem and Information Technology, Chinese Academy of Sciences, Shanghai 200050, China)

Abstract: The structure and main performance of InGaAs PIN detector are introduced. The progress of InGaAs detector, especially the key technology and main performance of InGaAs detector for space application of our country was reported. In recent years, InGaAs focal plane arrays (FPAs) have been developed rapidly to meet the requirements of space applications in our country. Both front side and backside illuminated 256×1 element linear InGaAs photodiode arrays have been fabricated for the 0.9 μm−1.7 μm spectra band. At room temperature, peak detectivity is 7.8×10^{11} cm·Hz$^{1/2}$/W and 4.5×10^{11} cm·Hz$^{1/2}$/W, respectively. Scanning images are obtained by using the front side one. The images are clear. Furthermore, the extended long-wavelength response InGaAs FPAs (~2.4 μm) with 256 elements are also developed, whose the peak detectivity is 2.5×10^{10} cm·Hz$^{1/2}$/W at room temperature. The research results provide a solid foundation for studying the longer linear FPAs. The performance needs further improvements for space application.

Key words: InGaAs; FPAs; Infrared detector; Space application

InGaAs

[1], [1,2], [1], [1,2], [1,2], [1,2], [1,2], [1],
[3], [3], [4], [1]

(1.   ,   200083；
2.   ，   100039；
3.   ，   130033；
4.   ，   200050)

:   InGaAs PIN   ，   InGaAs   ，

InGaAs   。   ，

InGaAs   ，   0.9~1.7 μm   256×1

InGaAs   ， 7.8×10^{11} cm·Hz$^{1/2}$/W 4.5×10^{11} cm·Hz$^{1/2}$/W，

256×1   InGaAs   ，   。   ，

2.4 μm   256×1   InGaAs   , $2.5×10^{10}$ cm·$Hz^{1/2}$/W。

,

,   。

：InGaAs；   ；   ；

0 Introduction

1－3 μm infrared technology has wide applications in spatial remote sensing since many substances have special spectra characteristics in this waveband, such as the hydroxyl in rocks and minerals, the water in crops, CO_2, NH_3, H_2S and N_2O in the atmosphere. Moreover, infrared radiations from many high temperature substances, such as the engine spout of planes and rockets, the tail flames of missiles, also cover in this band. Therefore, short wavelength infrared (SWIR) focal plane arrays (FPAs) could be widely used in space-to-ground detection in many military and commercial fields such as military reconnaissance and monitoring, crop assessment, resource distribution, soil moisture inspection and atmospheric composition analysis[1-2].

HgCdTe and InGaAs are two main materials used to fabricate SWIR detectors. HgCdTe FPAs usually need to be cooled to restrain its thermal noise, but the cooler would greatly increase the power consumption and bulk of the infrared systems, and the thermal stress under low temperature may lead to device degeneration, even failure, thus affect the system performance and service lifetime. There is an increasing demand for high performance infrared detectors. It is reported that, InGaAs detector has higher performances than HgCdTe detector in the spectral band below 2.5 μm. Therefore, many countries compete in developing the InGaAs FPAs.

After several years′ development, many satellites used infrared spectrometers with the InGaAs FPAs in space applications. These satellites include the earth observation satellite EO－1, which used a 256×256 InGaAs FPAs with pixel size of 40 μm×40 μm and a response wave band of 0.9－1.6 μm; the SPOT4 and SPOT5 satellite with a 3 000 element linear InGaAs SWIR scanning FPAs [3]; the environment satellite ENVISAT, which used a 1 024 element linear InGaAs FPAs in the four channels on its core SCIAMACHY

(Scanning Imaging Absorption spectroMeter for Atmospheric CartograoHY), and this is the first application of extended long-wavelength response InGaAs detectors in satellite [4]; the moon observation satellite SELENE, which used un-cooled 320×240 element planar InGaAs arrays with 40 μm×40 μm pixel areas.

In this paper, the basic properties of InGaAs are introduced, and the quantum efficiency, dark current and noise of the InGaAs detector are theoretically analyzed. Both front side and backside illuminated InGaAs photodiode arrays with mesa structure are successfully fabricated for space applications, and their performance is introduced.

1 Basic properties of InGaAs

The direct band gap ternary compound $In_xGa_{1-x}As$ is III－V group pseudobinary semiconductors with high electron mobility and good antiirradiation characteristics. As shown in Fig.1, the band gap of $In_xGa_{1-x}As$ could vary from 0.35 eV of InAs to 1.43 eV of GaAs, corresponding to the cut-off wavelength 3.5 μm and 0.87 μm, respectively. That is to say, the cut-off wavelength could be changed by modulating x. $In_{0.53}Ga_{0.47}As$ is completely lattice-matched to InP material, and high quality epitaxial layer could be grown on InP substrates to fabricate devices with excellent performance. By increasing the content of In,
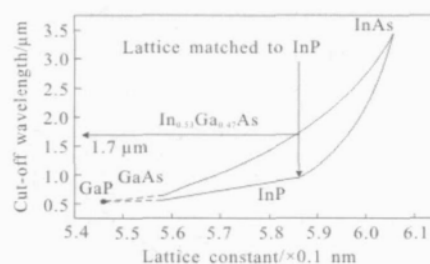

Fig.1 Relationship between the lattice constant and the long cut-off wavelength of the 4 ternary in the InGaAsP family

the response band of In$_x$Ga$_{1-x}$As will extend to long wavelength. The InGaAs photodiode arrays can work under room temperature, and extended long -wavelength response InGaAs photodiode arrays could acquire favorable performance under pyroelectric cryogenic conditions. Therefore, InGaAs detectors could get rid of limitation of low temperature cooling, and have great competence in device miniaturization and infrared system cost.

2 Theoretical analyses

For the p -i -n photodiode is easy to be fabricated and can acquire high performance, many research institutes resort to this kind of structure to fabricate InGaAs photodiode arrays for space application.

The p -i -n structure photodiode works using the photovoltaic effect of p -n junction, the electrons and holes induced by light radiation drift under strong electric field and produces photo -current in the external circuit. The device performance is mainly determined by the quantum efficiency and dark current.

2.1 Quantum efficiency

The quantum efficiency η is the probability that a photoelectron is produced when a photon is incident on the detector. For an incident optical power Φ_p, which produces a photocurrent $I_p = R\Phi_p$, here R is the responsivity. The quantum efficiency is calculated from

$$\eta = \frac{\left(\dfrac{I_p}{q}\right)}{\left(\dfrac{\Phi_p}{h\nu}\right)} = \frac{h\nu}{q}R \tag{1}$$

where q is the elementary charge, h is the Planck constant and ν is the photon frequency.

2.2 Dark currents

Four mechanisms can be identified in dark currents of the photovoltaic device: the minority -carrier diffusion current, the generation -recombination current in the barrier region, the surface leak current brought by surface damage, and the direct and indirect tunneling current arising from deep energy level. The dark currents of the photodiode used in space application limit the device sensitivity, so the dark current should be as low as possible.

The different current mechanisms are described as follows. The surface leak current density is

$$J_{if} = \frac{q}{2} n_i \sqrt{\sigma_n \sigma_p}\, v_{th} N_{is}\, \pi k_B T \tag{2}$$

where n_i is the intrinsic carrier concentration, v_{th} is the mean free -carrier velocity, N_{is} is the surface state density, σ_n and σ_p are the capture cross -sections of electron and hole, respectively, and related with detector material and doping. Note that the surface leak current density is independent on reverse -bias voltage.

The diffusion current density can be expressed as

$$J_{diff} = \frac{q n_i^2}{N_D} \sqrt{\frac{D_p}{\tau_p}} \left[\exp\left(\frac{-qV_{bias}}{k_B T} \right) - 1 \right] \tag{3}$$

where D_p is the diffusion constant for holes , τ_p is the hole lifetime, N_D is the donor concentration, V_{bias} is the reverse -bias voltage and the remaining symbols have the usual meaning. Note that the diffusion current has strong temperature dependence because the intrinsic carrier concentration n_i increased rapidly with the temperature.

The generation -recombination current density can be expressed as

$$J_{g-r} = q \frac{n_i W}{\tau_{eff}} \left[\exp\left(\frac{-qV_{bias}}{k_B T} \right) - 1 \right] \tag{4}$$

where W is the depletion width and τ_{eff} is the effective carrier lifetime. Note that the generation -recombination current can be reduced by decreasing the depletion width and increasing the effective carrier lifetime.

The tunneling current density can be expressed as

$$J_{tun} = \frac{q^3 F_m V_{bias}}{h^2} \sqrt{\frac{2m_e}{E_g}} \exp\left[\frac{-8\pi}{3qF_m h} \sqrt{2m_e E_g^3} \right] \tag{5}$$

where F_m is the electric field at the p -n junction , and the remaining symbols have the usual meaning. The tunneling current is proportional to the bias current, and weakly depends on the temperature.

As known from above analysis, we can effectively decrease the dark current and improve device properties by properly controlling material doping level, decreasing the material defects, improving the surface processing and passivation technology.

3 Progress of InGaAs FPAs

3.1 Front side illuminated InGaAs photodiode arrays

There are two types of InGaAs photodiode arrays, front side and backside illuminated devices. A front side illuminated InGaAs device with a 256 element array had been fabricated by G. H. Olsen [5]. The InGaAs photodiode arrays have been configured into linear arrays of 30 μm $\times$30 μm with 50 μm spacing. The devices have typical responsivity of 0.9 A/W (86% quantum efficiency) at 1.3 μm and exhibit room temperature dark currents below 100 pA. Wafers of InGaAs/InP were fabricated via hydride vapor phase epitaxy (VPE) with the structure shown in Fig.2 A planar process consisting of silicon nitride deposition, zinc diffusion and gold/zinc metallization was to form a detector active area.
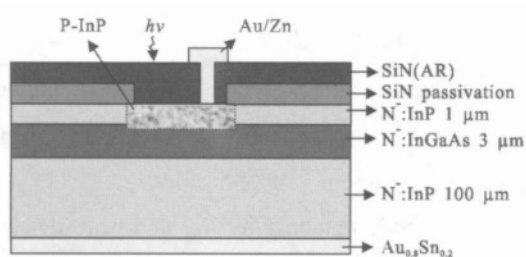

Fig.2 Cross-sectional sketch of a planar InGaAs/InP photodiode for 0.8−1.7 μm response

The InGaAs photodiode arrays used in the FPAs are based on standard p-i-n photodiodes. They are fabricated using the planar or mesa structure. The mesa structure devices have simple fabrication processing and little cross-talk between neighboring pixels. Based on the mesa structure, we developed the front side illuminated InGaAs FPAs with a 256 element array for imaging from the 0.9 μm to 1.7 um for space applications. The FPAs consist of photodiode arrays, CMOS read-out circuits and thermoelectric cooler in a sealed package.

The photodiodes consist of three layers grown by molecular beam epitaxy (MBE) on an semi-insulated InP substrate, an InP buffer layer (n>2$\times$10^{18} cm^{-3}, 1 μm), an InGaAs absorption layer ($n \approx 2\times10^{16}$ cm^{-3}, 2.5 μm), and an InP cap layer (p>2$\times$10^{18} cm^{-3}, 0.5 μm)[6]. The

sample was firstly degreased in organic solvents. Then the photodiode array was obtained after mesa-making, SiN$_x$ passivation, growth of electrode. The structure of the photodiode is shown in Fig.3. The surface and sidewall of the detector are passivated by a SiN$_x$ layer, both the p and n contact are Ti/Pt/Au. Photograph of front side illuminated 256 $\times$1 element linear InGaAs photodiode arrays is shown in Fig.4.
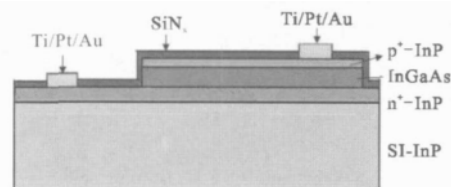

Fig.3 Cross-sectional sketch of a front side illuminated mesa InGaAs/InP photodiode

Fig.4 Photograph of 256$\times$1 element mesa InGaAs photodiode arrays

The readout integrated circuit (ROIC) is an important part of FPAs, it consists of unit cell electronics that provide the detector bias, photocurrent integration (i. e. charge-to-voltage conversion), pixel selection, and peripheral electronics for addressing the unit cell electronics, external interfacing and additional output buffering. The capacitance feedback transimpedance class of amplifier (CTIA) is a reset integrator and addresses a broad range of detector interface and performance requirements across many applications. It provides low input impedance and a constant detector voltage. It has very low noise from low to high backgrounds. Signal processing such as correlated double sampling (CDS) is often employed on the output of the CTIA, within the unit cell, primarily to reduce drift but also to re-reference the output signal to a more convenient voltage range. CDS is used to suppress the kTC noise generated by resetting the feedback capacitor. This CDS involves sampling each pixel twice, once at the beginning of the frame and again at the end, and subtracting the difference. CDS also can be used to reduce 1/f noise and fixed pattern noise (FPN)[7]. Based on the CTIA unit cell as shown in Fig.5, the ROICs
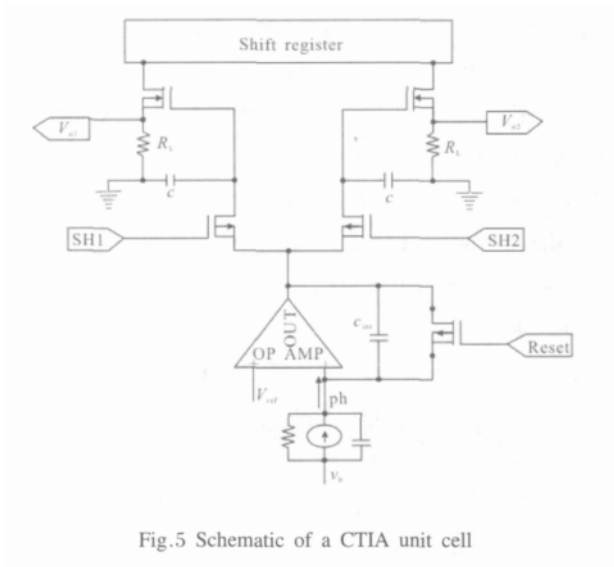
Fig.5 Schematic of a CTIA unit cell

were designed and fabricated.

The photodiode arrays were packaged in 32 -pins, dual -in -line package in nitrogen gas by parallel sealing, as seen in Fig.6. Thermoelectric cooler was joined in the package by tin soldering. A sapphire substrate carries two ROICs and InGaAs photodiode arrays, which were bedded on the thermoelectric cooler. The lid of the package contains a window of quartz glass. There are 256 wire bonds from the InGaAs photodiode arrays to the two circuits, 32 wire bonds from the circuits to substrate and 20 bonds from the substrates to pins.
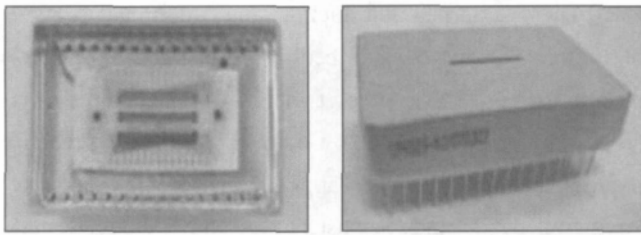

Fig.6 Assembly and package of 256×1 element mesa InGaAs FPAs

Signals of InGaAs FPAs were measured at room temperature. The integration time of the ROIC is 1 000 μs. The distance between blackbody and detector is 40 cm, and the temperature and aperture of blackbody as light source are 900 K and 1 cm, respectively. The response histogram of front side illuminated 256×1 element InGaAs FPAs with 1.7 μm cut -off wavelength is shown in Fig.7, and its noise histogram is shown in Fig.8. The response non - uniformity U_s is given by
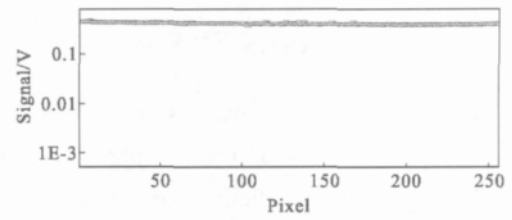
Fig.7 Histogram of response of 256×1 element mesa InGaAs FPAs(λ_c =1.7 μm)
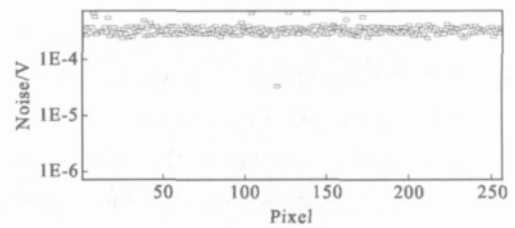
Fig.8 Histogram of noise of 256×1 element linear InGaAs FPAs (λ_c =1.7 μm)

$$U_s = \frac{1}{\overline{V_s}} \sqrt{\frac{1}{N-1} \sum_{i=1}^{N} \left(V_s - \overline{V_s} \right)^2} \qquad (6)$$

where $\overline{V_s}$ is the mean response signal, N is number of the diodes and V_s is the response signal. The response non -uniformity is about 4.8%.

The blackbody responsivity R_{bb} and peak detectivity $D_{\lambda_p}^*$ can be calculated by

$$R_{bb} = \frac{V_s \times 4L^2}{\sigma(T_2^4 - T_1^4) \times d \times A_D} \qquad (7)$$

and

$$D_{\lambda_p}^* = \frac{4GL^2 V_s \sqrt{1/2t_{int}}}{V_n \sigma(T_2^4 - T_1^4) d \sqrt{A_D}} \qquad (8)$$

respectively, where G factor is about 70, L is the distance between the black -body and the FPAs, T_2 is the tempe - rature of the black-body, T_1 is modulator temperature, V_s is the response signal, t_{int} is the integration time, V_n is the noise, σ is the Stefan constant, d is the aperture of black- body, and A_D is the photoactive area of the photodiode. The blackbody responsivity R_{bb} is 2.3×10^9 V/J, and the peak detectivity $D_{\lambda_p}^*$ is 7.8×10^{11} cm·Hz$^{1/2}$/W. The scanning system was set up, and the clear photograph was obtained as shown in Fig.9[8–10].

Fig.9 Scanning photograph of 256×1 element mesa InGaAs FPAs

3.2 Backside illuminated InGaAs photodiode arrays

Backside illuminated structure is suitable for fabricating large-scale two-dimensional devices. Martin H. Ettenberg et al demonstrated a 640×512 InGaAs FPAs with 25 μm pixels for a total size exceeding 2 cm². The device is sensitive to the 0.9−1.7 μm short wave infrared band and features a room temperature detectivity greater than $5×10^{12}$ cm·Hz$^{1/2}$·W^{-1} with greater than 98% of the pixels operable [11].The device process is shown in Fig.10. Fig.10 (a) illustrates the epitaxial structure. The photo-diode array is based on a standard p-i-n photodiode. The surface of the wafer was passivated with a coating of SiN$_x$ as seen in Fig.10 (c). Through standard photolit-hography techniques, holes were opened in the Si$_3$N$_4$ coating through plasma etching. The holes allowed zinc diffusion, typically using a ZnAs or ZnP source. The Zn diffused through the InP cap to the InGaAs active layer as seen in Fig.10 (e), which defined the junctions. A second layer of SiN$_x$ was applied to protect the newly exposed semiconductor surface. "Streets" were etched around each photodiode array down to the n-substrate. This allowed p$^+$ and n$^+$ contacts to be formed on the epitaxy side of the structure, and all of the contacts to be placed on one side while the other side was optically unobstructed. Holes were defined in the SiN$_x$ layer over each pixel and Au/Zn p-type ohmic contacts were deposited as can be seen in Fig.10 (b). Au/Ge n-type contacts were deposited in the "streets". Metal overlays were deposited to bring the substrate contacts in the "streets" to the top surface of the die so all of the contacts were at the same height and thus in the same plane, as seen in Fig.10 (d). The final step was to deposit indium bumps on each pixel, showed in Fig.10 (f). These bumps allowed the contact between the multiplexer and the photodiode array. Sensors Unlimited is the famous
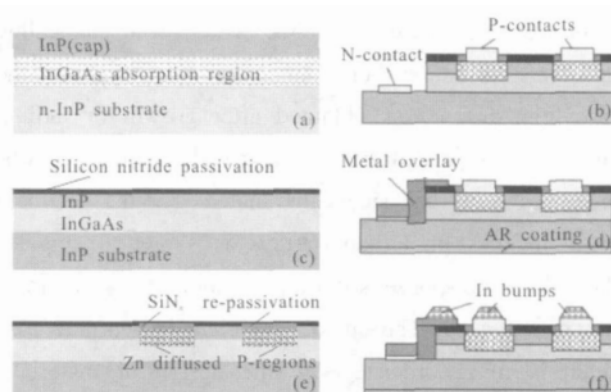

Fig.10 Fabrication of backside illuminated planar InGaAs photodiode arrays

company for providing InGaAs FPAs. In 2005, they demonstrated two types of arrays with more than one million detector elements—one with 1 024×1 024 elements and the other with 1 280×1 024 elements for low background applications. The detector elements of both formats were on a 20 μm pitch. The typical zero bias resistance-area product $R_0A=1.5×10^7$ Ωcm², which ensure the high performance of the InGaAs FPAs in passive night vision system[12−13].

Based on the mesa structure, we developed the backside illuminated InGaAs FPAs with a 256 element array for imaging from the 0.9 μm to 1.7 μm for space applications. The epitaxy structure of the photodiode array consists of a 0.6 μm p-InP top layer with the carrier concentration of $2×10^{18}$ cm^{-3}, a 1.5 mm i-In$_{0.53}$Ga$_{0.47}$As absorption layer with the carrier concentration of $3×10^{16}$ cm^{-3} and a 0.5 μm n-InP buffer layer with the carrier concentration of $2×10^{18}$ cm^{-3}. The wafers were processed into mesa type photodiodes, as seen in Fig.11. Photosensitive areas were defined as 25 μm×25 μm by photolithography and etching, and then passivated using the SiN$_x$ film. The top and
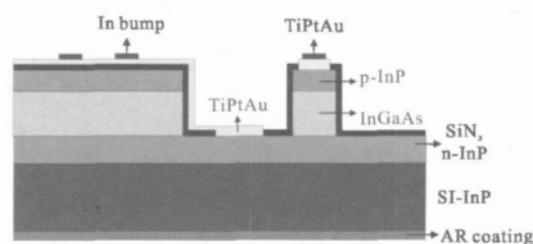

Fig.11 Fabrication of backside illuminated planar InGaAs photodiode arrays

bottom contact were Ti/Pt/Au, which were annealing for the formation of ohmic contact. Then the photodiode array was obtained after growth of indium bumps, substrate polishing and growth of a AR layer. Photograph of backside illuminated 256 ×1 element linear InGaAs photodiode arrays is shown in Fig.12. The relative response spectrum at room temperature is shown in Fig.13. The cut-off wavelength is at 1.7 μm, which is in accordance with the design of materials. Due to the absorption of the InP substrate, the photodiode array has good cut-off characteristics in short wavelength direction.

Fig.12 Photograph of 256×1 element backside illuminated mesa InGaAs photodiode arrays
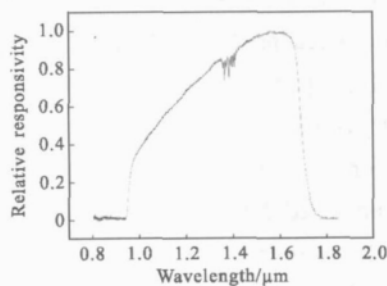

Fig.13 Response spectrum of backside illuminated mesa InGaAs photodiode arrays

The back side InGaAs FPAs consist of photodiode arrays, CMOS read-out circuitry and thermoelectric cooler in a sealed package. The integration time of the ROIC is 3 000 μs. The distance between blackbody and detector is 40 cm, and the temperature and aperture of blackbody as light source are 900 K and 1 cm, respectively. The response histogram of backside illuminated 256 ×1 element InGaAs FPAs is shown in Fig.14, the peak
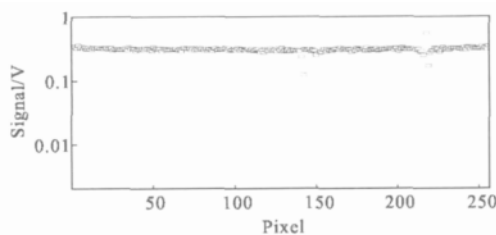

Fig.14 Response histogram of 256×1 element backside illuminated mesa InGaAs FPAs(λ_c=1.7 μm)

detectivity is 4.5×10^{11} cm·Hz$^{1/2}$/W with greater than 98% of the pixels operable.

3.3 Extended long-wavelength response InGaAs FPAs

The 1.5−2.5 μm spectra is of interest for infrared detector applications such as eyesafe rangefinding, LIDAR (both atmospheric pollution and windshear monitoring), chemical spectroscopy and flame detection at 2.55 μm. Linear and two-dimensional arrays of detectors can be applied to satellite imaging for remote sensing, resource management and spectroscopy in the same spectral region.

In order to grow $In_xGa_{1-x}As$ absorption layers with longer wavelength response, the so-called grading layer technique is employed to accommodate the large lattice parameter mismatch between the InP substrate and the absorption layer. The graded layer can prevent the propagation of mismatch dislocation from layer to layer. In this way, it is possible to grow epitaxial material with high performance. Fig.15 shows a grading layer structure. Here the mismatch is accommodated by a number of abrupt $InAs_yP_{1-y}$ layers, where the value of y increases from layer to layer. The extended long-wavelength response InGaAs FPAs with 1 024 phot-odiode arrays had been used in SCIAMACHY instru-ment of ESA′s environmental satellite. The geometry of the pixels is 500 μm×13 μm, on 25 μm spacing. In -10 mV bias voltage, the mean dark current is 30 nA at room temperature.
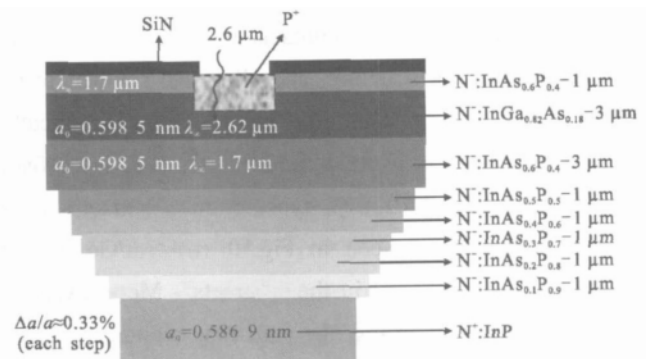

Fig.15 Schematic cross-section of the 2.6 μm photodiode

Aiming at space application, we fabricated the extended long-wavelength response InGaAs photodiode arrays with front side illuminated structure using gas source molecular beam epitaxy (GSMBE) materials.

The material was grown with indium gallium arsenide ($In_xGa_{1-x}As$) grading layers, whose structure is shown in Fig.16. The low-bandgap heavily-doped cap layer is used as a contact layer, with a low sheet resistance to minimize series resistance. This cap layer is thin enough to minimize light absorption in this region. We preferred to use an $In_xGa_{1-x}As$ grading layer rather than an $InAs_xP_{1-x}$ grading layer, because it was easier to grow by MBE technique. The practical approach was to adjust the lattice constant in linear transformation, from the value of the InP substrate to the value of the $In_xGa_{1-x}As$ (x=0.78), by adjusting indium content value x of the buffer layers.
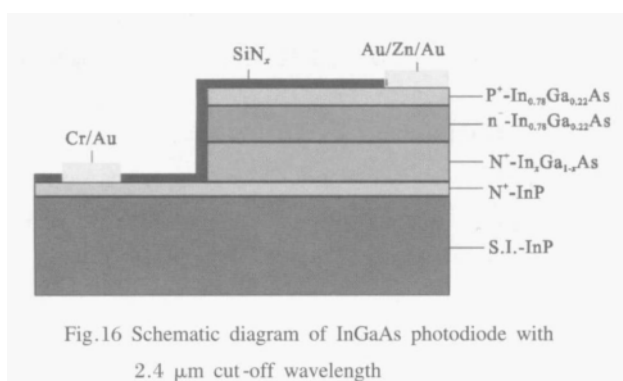

Fig.16 Schematic diagram of InGaAs photodiode with 2.4 μm cut-off wavelength

The wafer was degreased in organic solvents, and then dipped in concentrated HF for 10 s to remove the native oxides. After that, the mesa was realized by etching up to the n^+−InP buffer layer for device isolation using Ar^+ plasma and chemical etching. Then the wafer was dipped into a solution of $(NH_4)_2S_x$ for 30 min at 60 °C, followed by rinsing in deionized water and blow-dried using nitrogen before loading into the PECVD chamber for deposition of a SiN_x layer [14−15]. Finally, n-type metal contacts were realized by sputtering Cr/Au; p-type metal contact was realized by evaporating Au/Zn/Au using the e-beam evaporation technique, and the good contact was achieved by annealing at 450 °C for 15 s. The response spectra InGaAs photodiode arrays are shown in Fig.17. The cut-off wavelength of the standard and the longer wavelength response InGaAs photodiode arrays is 1.7 μm and 2.4 μm, respectively. The response non-uniformity and mean detectivity of the InGaAs FPAs with 2.4 μm cut-off wavelength are 10% and 2.5×

10^{10} cm·$Hz^{1/2}$/W, respectively. The 1/f noise inflexion is below 100 Hz[16].
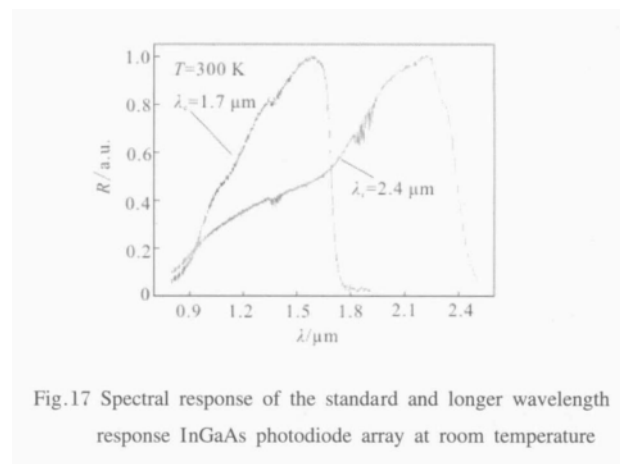

Fig.17 Spectral response of the standard and longer wavelength response InGaAs photodiode array at room temperature

3.4 Extended short-wavelength response InGaAs FPAs

In practical applications, InGaAs is expected to be used in both SWIR and visible imaging, even in UV imaging. A common method is to reduce the thickness of the cap or substrate InP layer. J. Barton et al had developed a method for processing standard InGaAs detector material. This method enhanced the short wavelength spectral response, extending the cut-on wavelength down to 350 nm [17−19]. Standard InGaAs FPAs are typically finished with an anti-reflection (AR) coating, however, in order to reduce the reflection induced loss in visible range, this improved InGaAs detector was fabricated with no AR coating. J. Barton et al also presented the imaging pictures from the standard and improved InGaAs photodiode arrays. The improved InGaAs detector can distinguish the details of the objects, but the standard one can't. This kind of detectors has preferable application prospects in space applications.

4 Conclusions

In the paper, the research progresses of InGaAs FPAs are reviewed. In space application, the mostly used ones are $In_{0.53}Ga_{0.47}As$/InP FPAs with 0.9−1.7 μm response spectrum. There are also great developments in the InGaAs FPAs extended to short and long wavelength response with preferable application

prospects. The short wavelength infrared wave band detection technology has important application in space application. The key is to improve the performance of SWIR detectors. With the development of IR FPAs in commerce, military and space applications, the InGaAs FPA s will develop to large scale, multi -colors, low power consumption, miniaturization and integration in the future.

References:

[1] HANSEN M P, MALCHOW D S. Overview of SWIR detectors, cameras, and application[C]//**Proceedings of SPIE, Thermos -ense XXX**,2008,**6939**:693901.

[2] CHEN Hong -jun, ZHOU Hang -yu. Recent progress in InGaAs visible/short wavelength infrared focal plane array detectors [J]. **Infrared and Laser Engineering**,2007,**36**(4):431−434.

[3] MOY J P, HUGON X, CHABBAL J, et al. 3000 InGaAs photodiode multiplexed linear array for SPOT4 SWIR channel [C]//**Proceedings of SPIE, Infrared Detectors, Focal Plane Arrays, and Imaging Sensors**,1989,**1107**:137−151.

[4] HOOGEVEEN R W M , van der A R J, GOEDEA P H. Extended wavelength InGaAs infrared (1.0 −2.4 μm) detector arrays on SCIAMACHY for space -based spectrometry of the Earth atmosphere[J].**Infrared Physics & Technology**,2001,**42**:1−16.

[5] OLSEN G H, JOSHI A M, BAN V S, et al. Multiplexed 256 element InGaAs detector array for 0.8 μm −1.7 μm room temperature operation [C]//**Proceedings of SPIE, Wave Pro -pagation and Scattering in Varied Media**,1988,**972**:279−285.

[6] LV Yanqiu, WANG Nili, ZHUANG Chunquan, et al. The uniformity of InGaAs in InP/InGaAs/InP by microwave photoconductivity decay (μ -PCD) carrier lifetime measurement [J].**Semicond Sci Technol**,2006,**21**:771−774.

[7] FOSSUM E R, PAIN B. Infrared readout electronics for space sensors: state of the art and future directors[C]//**Proceedings of SPIE,Infrared technology XIX,**1993,**2020**:262−282.

[8] TANG Hengjing, WU Xiaoli, ZHANG Kefeng, et al. High uniformity InGaAs linear mesa -type SWIR focal plane arrays [C]//**Proceedings of SPIE,Infrared Materials, Devices, and Applications**,2007,**6835**:683516.

[9] LV Yan -qiu, HAN Bing, BAI Yun, et al. 256 elements InGaAs linear IR focal plane array and scanning image[J].**J Infrared Millim Waves**,2008,**27**(1):7−11.(in Chinese)

[10] GONG Hai -mei, ZHANG Ke -feng, TANG Heng -jing, et al. Developments of near IR linear InGaAs FPAs in China [J]. **Infrared and Laser Engineering**,2009,**38**(1):14−18.(in Chinese)

[11] ETTENBERG M H, LANGE M J,O′GRADY M T, et al. A room temperature 640×512 pixel near -infrared InGaAs focal plane array[C]//**Proceedings of SPIE, Infrared Detectors and Focal Plane Arrays VI**,2000,**4028**:201−207.

[12] HOFFMAN A, SESSLER T, ROSBECK J, et al. Megapixel InGaAs array for low background applications[C]//**Proceedings of SPIE, Infrared Technology and Applications XXXI**,2005, **5783**:32−38.

[13] BOISVERT J, ISSHIKI T, SUDHARSANAN R, et al. Perfor -mance of very low dark current SWIR PIN arrays [C]// **Proceedings of SPIE, Infrared Technology and Applications XXXIV**,2008,**6940**:69400L.

[14] TANG H J , WU X L, XU Q F, et al. Effect of sulfur passivation on the InP surface prior to plasma -enhanced chemical vapor deposition of SiNx [J].**Semicond Sci Technol**, 2008,**23**:035031.

[15] TANG H J, WU X L, ZHANG K F, et al. The defect density of a $SiN_x/In_{0.53}Ga_{0.47}As$ interface passivated using $(NH_4)_2S_x$ [J]. **Applied Physics A**,2008,**91**:651−655.

[16] ZHANG Kefeng, TANG Hengjing, WU Xiaoli, et al. Perfor -mance analysis of 256 element linear 2.4 μm InGaAs photovoltaic detector arrays[C]//**Proceedings of SPIE, Infrared Materials, Devices, and Applications**,2007,**6835**:683506.

[17] HOELTER T R, BARTON J B. Extended short wavelength spectral response from InGaAs focal plane arrays [C]// **Proceedings of SPIE, Infrared Technology and Applications XXIX**,2003,**5074**:481−490.

[18] ENRIQUEZ M D, BLESSINGER M A, GROPPE J V, et al. Performance of high resolution visible -InGaAs imager for day/ night vision [C]//**Proceedings of SPIE, Infrared Technology and Applications XXXIV**,2008,**6940**:69400O.

[19] TURNER D G, BAKKER T C, DIXON P, et al. The development of, and application for, extended response (0.7 to 1.7 μm) InGaAs focal plane arrays [C]//**Proceedings of SPIE, Infrared Technology and Applications XXXIV**, 2008,**6940**:694037.